Intelligent detection of melanoma growth stage based on the analysis of the thermal response of skin

Fatemeh Khosravi

Department of Mechatronics Engineering,
University of Tabriz,
P.O. Box 5166616471, Tabriz, Iran
Email: ftm.khosravi68@gmail.com

Mohammad-Reza Sayyed Noorani*

Rehabilitation Robotics Research Lab,
Department of Mechatronics Engineering,
University of Tabriz,
P.O. Box 5166616471, Tabriz, Iran
Email: smrs.noorani@tabrizu.ac.ir
*Corresponding author

Maryam Shoaran

Artificial Intelligent Research Lab,
Department of Mechatronics Engineering,
University of Tabriz,
P.O. Box 5166616471, Tabriz, Iran
Email: mshoaran@tabrizu.ac.ir

Abstract: In response to a thermal stimulation, skin tumours produce different temperature variations in comparison with healthy tissues. In this paper, we exploit this fact to design an intelligent melanoma detection system that estimates the development stage of a skin tumour. This system is based on a feed-forward artificial neural network, which receives a signal of the thermal response measured from the skin surface, and predicts the growth stage of the tumour. The measurement should be performed during the heat recovery after removing a cold stimulus. In order to train and test the neural network, here, these signals are provided by FEM-based simulations that solve the Pennes' bioheat transfer equation. Also, the signals are processed quantitatively and their convenient features are extracted. The achieved accuracy of 96% shows that the thermal response as the distinguishing criterion is an appropriate choice for the early diagnosis of the melanoma type of skin cancer.

Keywords: intelligent systems; artificial neural networks; ANNs; melanoma early diagnosis; Pennes' bio-heat transfer equation.

Reference to this paper should be made as follows: Khosravi, F., Noorani, M-R.S. and Shoaran, M. (2020) 'Intelligent detection of melanoma growth stage based on the analysis of the thermal response of skin', *Int. J. Biomechatronics and Biomedical Robotics*, Vol. 3, No. 4, pp.188–196.

Biographical notes: Fatemeh Khosravi received her BSc in Electrical Engineering from the University of Shahrekord, Iran in 2012. She received her MSc in Mechatronics Engineering from the School of Engineering – Emerging Technologies, University of Tabriz, Iran in 2016. At the present, she is an Instructor at the Department of Mechanics, University of Shahrekord, Iran. She is a member of Iranian Society of Mechatronics. Her research interests include Mechatronics, Electrical, and Biomedical Engineering.

Mohammad-Reza Sayyed Noorani received his BSc in Mechanical Engineering from the Sharif University of Technology, Engineering College at Golpayegan, Iran in 2006 and MSc and PhD in Mechanical Engineering from the University of Tabriz, Iran in 2009 and 2013, respectively. At the present, he is an Assistant Professor of Mechatronics Engineering at the University of Tabriz. His research interests are in the areas of biologically inspired robotics, rehabilitation robotics, dynamics, control, and system identification.

Maryam Shoaran first studied medicine from 1990 to 1992, however, by pursuing her interest in computer science, she changed her field of study in 2001 and received her BSc in Computer Engineering from the Shahid Beheshti University, Tehran, Iran in 2005. She received her MSc

and PhD in Computer Science from the University of Victoria (UVic), Canada in 2007 and 2011, respectively. After two years of Postdoctoral Research at the UVic, she came back to Iran and currently works as an Assistant Professor at the Department of Mechatronics Engineering, University of Tabriz, Tabriz, Iran.

1 Introduction

Cancer is a disease in which the cells do not grow in the normal course of the growth, which leads to the seizure, destruction, and deterioration of healthy tissues. Skin cancer is the most common type of cancer, with the rate of about 75% of all cancers worldwide. This type of cancer exists in both epidermis and dermis layers, and is divided into melanoma and non-melanoma. Melanoma has access to both lymphatic system and blood vessels through skin, and invades healthy cells quickly (Liu, 2008; Çetingül and Herman, 2011; Keangin et al., 2011). Therefore, the diagnosis of melanoma in early stages of the growth in a simple, accessible, and repeatable way is the concern of many physicians in this field, with the goal of starting timely remedial treatments (Agnelli et al., 2011; Elder, 1999).

Of the conventional methods for an early diagnosis of melanoma are:

1 examination of visual features with naked eyes

2 using the extraction of subsurface features, for example, by dermoscopy

3 surgical excision to determine the cause and circumstances of the tumours growth.

In addition, pathological studies as a medical protocol should be considered before any decision. Apart from the advanced conventional methods, in the past few years a growing role of thermometry (thermography) for subsurface cancer has been witnessed. Thermometry is relatively simple, inexpensive, usable in the clinic, and repeatable. Therefore, further research to develop new methods for the early detection of melanoma using thermometry, and evaluation of the ability of this approach seems to be essential in the diagnosis (Qi et al., 2008).

Medical studies have shown that in the areas of tumour growth, blood perfusion rate dramatically increases. Moreover, often the metabolism rate of healthy cells in the neighbourhood of the tumour goes up abnormally. These factors cause the skin surface temperature, at the top of the tumour, to have different values than the healthy tissue surrounding the tumour in each stage of melanoma growth. The differences in the thermal response of the healthy and diseased areas with respect to an external thermal stimulation can be exploited as an indicator for the early detection of cancer cells. The analysis of bioheat transfer equation in the skin tissue produces useful data that can be acquired from the distinctive thermal behaviour of healthy and cancerous cells. These data may be utilised to design an intelligent classifier system. By this method, we can provide a great help in the diagnosis and determination of cancer extent (Singh and Kumar, 2014). Of the strongest classification methods are artificial neural networks (ANNs), which are widely used for identification and evaluation in expert systems including disease detection systems. Smart medical systems based on ANNs have been used for the diagnosis of cancer, cardiovascular disease, tuberculosis, and sinus infections. The advantage of using intelligent systems for disease diagnosis is that the mal effect of the factors such as confusion, fatigue, anxiety, or emotional feelings of the physician conducting the medical examination or test on the diagnosis is minimised.

To design an intelligent system for melanoma detection using the skin thermal response, it is necessary to first identify the equation governing the heat energy balance in the skin tissue. The thermal behaviour of the skin has been studied using the Pennes' bioheat transfer equation by many researchers, which we review few of them in the following.

Deng and Liu (2004) used the Monte-Carlo method to solve the Pennes' equation in a three-dimensional domain with nonlinear boundary conditions. They simultaneously considered various factors such as convection, surface evaporation, and radiation on the skin. The results showed that the temperature in the region of the tumour growth is higher than healthy regions. Dehghan and Sabour (2012), also based on Deng and Liu's (2004) research, worked on the numerical solution of Pennes' equation by using a spectral element method. This research includes a limited area of two-dimensional model with three separate layers of skin that the cancerous cells have been placed in the area. Their obtained results were similar to the results presented by Deng and Liu (2004). Singh and Kumar (2014) studied heat wave equation numerically in a three-layer model of the skin during freezing. They considered two time delays in their model, a delay for the thermal flux and the other for the temperature distribution. Using two time delays was due to consider the impact of micro-scale structure in the transient heat transfer. In common models established upon the parabolic differential equations, this difference in delays is not considered (Ströher and Ströher, 2014). Ströher and Ströher (2014) analysed the problem of heat transfer on skin tissue and solved the problem numerically for both parabolic and hyperbolic approaches. These approaches extracted from the Pennes' equation where the mechanism of heat conduction assessed via classical Fourier law and non-Fourier law, respectively. Bhowmik et al. (2014) investigated a vascularised skin model to predict the thermal evaluation criteria of early melanoma using the dynamic thermal imaging (DTI) method. In this work, after applying cold stimuli, the temperature distribution during heat recovery on the skin surface in the presence of melanoma was presented. During the heat recovery, the skin was exposed to natural convection, radiation and evaporation. They predicted that the thermal response due to subsurface

blood flow overpowers the response of early melanoma and the diagnosis of melanoma at an early stage is immature.

Apart from the thermal analysis, other methods for the intelligent detection of melanoma have been presented in the literature. For instance, infra red (IR) imaging of the skin has been studied as a method of melanoma detection for many years (Mhaske and Phalke, 2013; Cetingül and Herman, 2010; Anbar, 1998; Cetingul, 2010; Jones, 1998; Jones and Plassmann, 2002; Herman and Cetingul, 2011; Cetingul and Herman, 2008). Mhaske and Phalke (2013) studied the performance of different classification methods, that is, SVM, neural networks, and clustering, in melanoma detection. The classifiers were based on features extracted from IR images. Using a multilayer computational model Cetingül and Herman (2010) showed that the surface temperature distributions are sensitive to both lesion width and penetration, while the effect of variations in thermophysical properties, like blood perfusion rate are negligible. Herman and Cetingul (2011) used specific image processing steps on dynamic IR images to accurately detect melanoma. Their system is based on thermal response difference between healthy and malignant tissue that relies on active cooling. In another work, Cetingul and Herman (2008) analysed the thermal response after cooling using a finite element model. They showed that the transient thermal response time during thermal recovery represents a broadly valuable information about the size and depth of any disruption in the skin.

In this paper, we design an intelligent system based on ANNs, which using the thermal response signals, it predicts the development level of a skin tumour with high accuracy. To the best of our knowledge, this is the first study that uses *intelligent learning methods* on *thermal response data* to detect melanoma. Most of the work in this area has been done using infra-red image analysis. For instance, among somewhat similar studies, Bhowmik et al. (2014) use DTI technique to detect and stage melanoma. Our results provide a quantified validation of Bhowmik et al. (2014) highlighting the effectiveness of thermal response/image analysis methods in skin cancer staging task. In another similar study, Mhaske and Phalke (2013) apply learning techniques on data extracted from infra-red imaging to only detect melanoma. Our results show a remarkable improvement in the accuracy of intelligent melanoma detection systems as well as staging the melanoma development.

In this study, first the thermal signals of 30 stages of the tumour growth, during thermal recovery after a controlled cold stimulus, are extracted via finite element method (FEM) simulations. Thermal process of the skin is modelled by Pennes' bioheat transfer equation. Then, these signals are processed and suitable features are extracted. Finally, a classifier is designed to accurately separate the stages of the melanoma development. Accuracy of 96% of the classifier represents the thermal response capability as a criterion for the diagnosis of melanoma in early growth stages of the disease.

2 Mathematical modelling

In Figure 1, a prismatic slice of human skin, which contains four main parts of epidermis, dermis, fat, and muscle, is schematically shown. In the centre of the x-y plane and near the skin top surface, an imaginary circular area is considered as the site of tumour growth. It is assumed that as the tumour grows, this circular area develops regularly in the depth and around the tumour. The model geometry and some thermal properties of the healthy tissue and melanoma are given in Table 1.

Figure 1 Five-layer structural model of skin including a melanoma lesion (dimensions in millimetres) (see online version for colours)

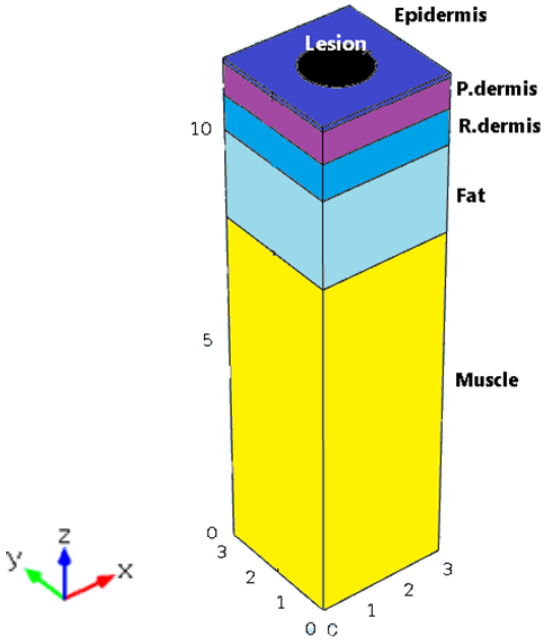

Staging of the growth of cancerous malignant tumours is determined based on the change in the effective diameter of the surrounding area and the depth of the lower layers (Bhowmik et al., 2014; Elder, 1999). Hence, in this study, the growth of melanoma has been modelled with respect to volume changes in the skin (i.e., expansion of peripheral and depth). Melanoma in early stages of its development (with a thickness of less than 1 mm) is known in the literature as melanoma T1. With the influx of melanoma T1 to healthy cells nearby, five-stage growth of the melanoma is followed, where the stages are called ESI, CLII, CLIII, CLIV, and CLV, respectively. In fact, we have considered the Clark levels, where the melanoma at its early stage before Clark levels is abbreviated as ESI. In Table 2, the diameter and the depth of the melanoma in some of its early stages of growth, along with corresponding cell metabolism and blood perfusion rate, are given. The data are used for simulating the thermal behaviour of the affected skin via Pennes' equation.

Table 1 Thermal properties of different layers of skin tissue as well as melanoma

Tissue layers	*Thickness (mm)*	C_t ($J\,kg^{-1}\,K^{-1}$)	K_t ($W\,m^{-1}\,K^{-1}$)	ρ_t ($kg\,m^{-3}$)	w_b ($m^3\,s^{-1}\,m^{-3}$)	Q_m ($W\,m^{-3}$)
Epidermis	0.1	3589	0.235	1200	0	0
Papillary dermis	0.7	3300	0.445	1200	0.0002	368.1
Reticular dermis	0.8	3300	0.445	1200	0.0013	368.1
Fat	2	2674	0.185	1000	0.0001	368.3
Muscle	8	3800	0.51	1085	0.0027	684.2
Melanoma	-	3852	0.558	1030	0.0065	3680

Source: Elder (1999)

Table 2 Change in diameter, depth, and thermal properties of the melanoma during its growth stages

Lesion	*Lesion diameter (mm)*	*Penetration depth (mm)*	*Blood perfusion ($m^3\,s^{-1}\,m^{-3}$)*	*Metabolic heat generation ($W\,m^{-3}$)*
L1	0.01	0.01	-	-
L2	0.1	0.1	-	-
L3	0.1	0.2	-	-
L4	0.15	0.215	-	-
ESI	0.2	0.22	-	-
L5	0.2	0.24	-	-
L6	0.24	0.24	-	-
L7	0.26	0.26	-	-
L8	0.28	0.26	0.0063	3680
L9	0.28	0.28	0.0063	3680
L10	0.32	0.3	0.0063	3680
L11	0.42	0.42	0.0063	3680
L12	0.52	0.44	0.0063	3680
CLII	0.68	0.44	0.0063	3680
L13	0.78	0.52	0.0063	3680
L14	0.88	0.64	0.0063	3680
L15	0.98	0.68	0.0063	3680
CLIII	1.0	0.7	0.0063	3680
L16	1.18	0.85	0.0063	3680
CLIV	1.28	1.0	0.0063	3680
L17	1.38	1.1	0.0063	3680
L18	1.48	1.2	0.0063	3680
L19	1.58	1.25	0.0063	3680
L20	1.68	1.34	0.0063	3680
L21	1.78	1.43	0.0063	3680
L22	1.88	1.53	0.0063	3680
L23	1.98	1.63	0.0063	3680
L24	2.08	1.74	0.0063	3680
L25	2.18	1.84	0.0063	3680
CLV	2.28	1.95	0.0063	3680

Source: Bhowmik et al. (2014)

The most common mathematical model to analyse the thermal behaviour of skin tissue is Pennes' bioheat transfer equation, which is extracted based on the conservation of heat energy in an element of the skin tissue. This equation can be expressed as follows:

$$\rho c \frac{\partial u(\mathbf{r},t)}{\partial t} = \nabla \cdot \left(k \nabla u(\mathbf{r},t)\right) + w_b \rho_b c_b \left(u_a - u(\mathbf{r},t)\right) + Q_m + Q_r(\mathbf{r},t) \quad (1)$$

where, the term on the left-hand side represents the energy storage per unit volume of skin, and on the other side, the first term is the thermal conductivity caused by the temperature gradient. The other terms are, respectively, the representative of the conventional heat transfer rate between skin tissue and blood flow, and the volumetric heat generated by cell metabolism due to the internal as well as space environmental heating. Also, u_a is the arterial blood temperature, and $u(\mathbf{r}, t)$ represent transients temperature distribution in the skin.

The Pennes' equation corresponding to each stage listed in Table 2 is solved numerically. Then, a set of thermal responses, that indeed are the temperature time histories, are achieved. Each of these responses is associated with a stage of early development of the melanoma. Thus, the difference in thermal response between normal and cancerous tissues, which simulated in various growth stages, can establish an information package. By comparing the thermal response of each suspected sample with samples of this package, the growth stage of the suspected sample in the early stages of disease can be estimated.

3 Numerical solution via FEM

To simulate the thermal response of the skin tissue with the melanoma lesion, we solve the Pennes' equation via FEM. The problem is solved each time using parameters corresponding to a stage of early development of the melanoma provided by Table 2. Then, numerical solutions are performed by COMSOL software in the region shown in Figure 2. It is assumed that the cancerous mass is located under the epidermis layer in a cylindrical area whose central axis is placed along that of the cubic region.

For simplification, the last term in equation (1) (i.e., space environmental heating term) is ignored. The thermal properties of the healthy and unhealthy areas are different. The blood perfusion rate (including factors related to heat transfer between the skin and the blood stream) and the heat rate of metabolism for each cubic and cylindrical area, in the early growth stages of melanoma, are set according to Table 2.

In this study, first we expose the skin uniformly to a cold stimulus with 10°C temperature for 60 seconds, and then the skin is released for natural convection at the ambient temperature considered 22.4°C. Thus, after the removal of the boundary condition of constant temperature in the upper face of the cube area (Dirichlet boundary condition), the skin is gradually recovered. During this heat recovery process, the thermal response on the skin surface will be evaluated. Figures 3 to 7 show the temperature differences between the thermal responses of the normal and cancerous samples evaluated in three stations of 30th, 120th, and 750th seconds after removing cold stimulus, for five chosen stages of the melanoma growth.

Figure 2 The meshed region containing the melanoma lesion, the COMSOL software (see online version for colours)

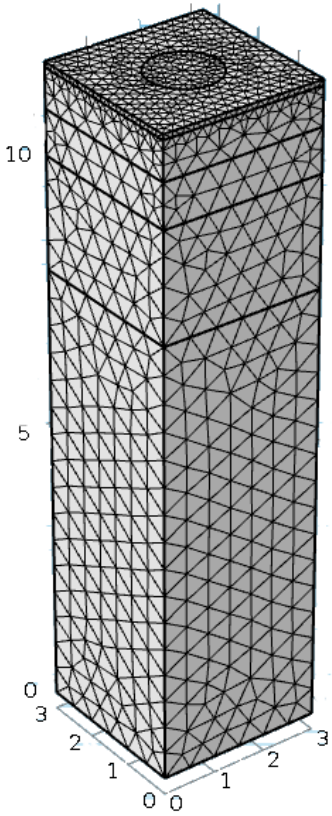

Our simulation results (partially depicted in Figure 3 to Figure 7), as predicted in Bhowmik et al. (2014) and Elder (1999), show that the temperature difference between the thermal responses of the healthy skin and the melanoma lesion during heat recovery increases with advancing stages of tumour growth. In all the stages (except for ESI that the effect of blood flow overcomes the early melanoma), the temperature difference reduces by time.

Figure 3 The temperature difference between thermal responses of healthy skin and melanoma lesion during heat recovery at the ESI stage of the tumour growth (see online version for colours)

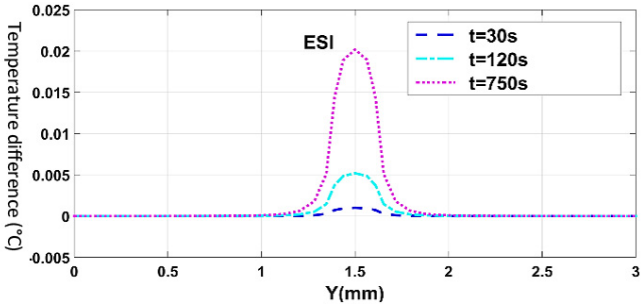

Figure 4 The temperature difference between thermal responses of healthy skin and melanoma lesion during heat recovery at the CLII stage of the tumour growth (see online version for colours)

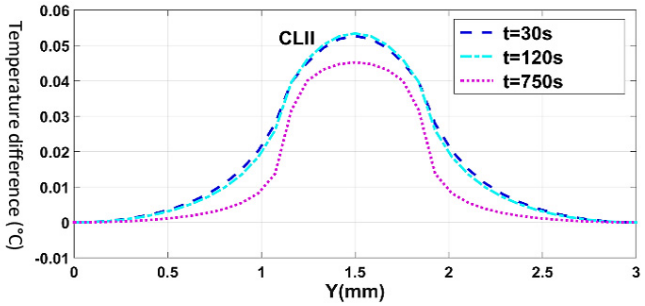

Figure 5 The temperature difference between thermal responses of healthy skin and melanoma lesion during heat recovery at the CLIII stage of the tumour growth (see online version for colours)

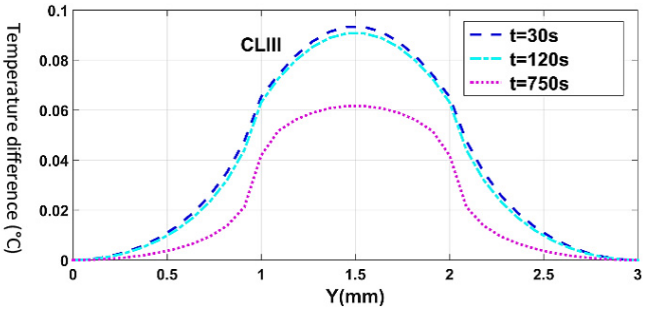

Figure 6 The temperature difference between thermal responses of healthy skin and melanoma lesion during heat recovery at the CLIV stage of the tumour growth (see online version for colours)

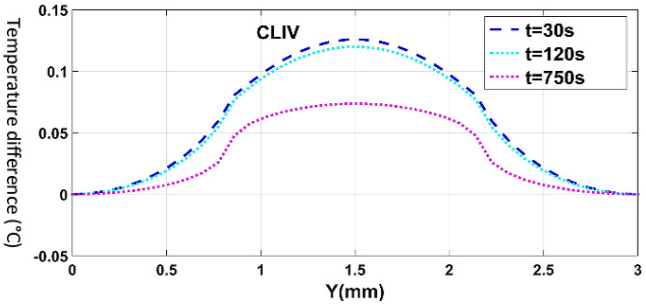

Figure 7 The temperature difference between thermal responses of healthy skin and melanoma lesion during heat recovery at the CLV stage of the tumour growth (see online version for colours)

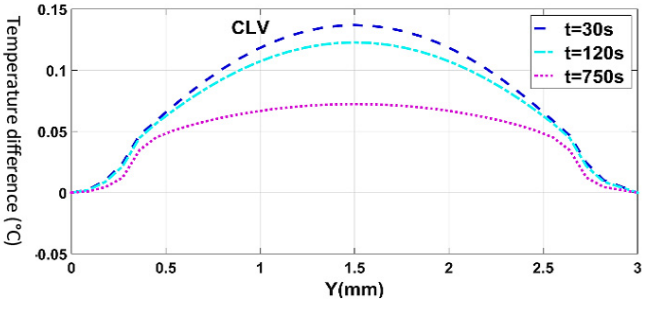

4 Classifier design

In the previous section by numerical solutions of Pennes' equation, thermal responses of melanoma in 30 steps of its early growth stages were simulated. Then, the difference between temperature distributions of the healthy and damaged tissues, during the heat recovery process after the removal of the controlled cold stimulus, was collected for every stage, to lastly establish an information package. The results show that the temperature differences at the growth stages of melanoma are different from each other and they are measurable. In addition, these differences are emphasised at the early time span of the heat recovery process. Therefore, it is reasonable that the thermal signals extracted a short time after the removal of the cold stimulus to be used for the detection of melanoma growth stage.

First, some indicators need to be specified in order to characterise the resulted thermal responses in a determined duration after removing the cold stimulus. Then, the information achieved from the two dimensional area on the skin surface is coded into these indicators. In this study to obtain indicators, each thermal response sample is first processed using Gaussian functions. Practically, using a Gaussian curve fitted to a time history, three features including its variance, area under the curve, and the peak of the temperature difference are extracted as indicators of the sampled thermal response. The signal processing phase is performed for the temperature difference distributions corresponding to all the simulated stages of the tumour growth. The signals are also taken from the first 30 seconds of the thermal responses after the removal of the cold stimulus (i.e., in the early of the heat recovery process).

For an intelligent inspection of a melanoma growth stage, a comparison can be carried out between the indexed thermal responses of the suspected sample and the samples provided in the information package. Clearly, if this comparison were to be made by an examiner it would be time-consuming and boring, and also, the resolution of detection which requires precise calculations would be beyond the scope of their capabilities. Hence, it is required to design an intelligent classifier.

In this study, we use a classifier based on ANNs. ANN classifiers have high power in separating data belonging to different groups. We use a supervised feed-forward neural network to detect the growth stage of a melanoma. In order to train the neural network (i.e., to adjust its weights), the well-known back-propagation algorithm is applied. We use the data from the simulated thermal responses as training data. Indeed, in each training step, the growth features extracted from a thermal response are given as the network input data, and expected output is the stage of the melanoma growth.

Figure 8 shows the schematic architecture of the designed three-layer neural network with input layer (1 × 3), a hidden layer with 15 neurons having *tansign* activation functions, and an output layer with five neurons having *softmax* functions. Therefore, the weight matrix will be 3 × 15 in hidden layer, and 15 × 5 in output layer. Table 3

gives the specifications of the network and the learning algorithm.

Designing and training the network is done by using the NN-toolbox of the MATLAB (see Table 3). As mentioned earlier, the indicators extracted from the difference between the thermal responses of healthy and damaged tissues at a certain growth stage, i.e., the temperature difference distribution variance (measured on the skin surface at the 30th seconds of the heat recovery), area under the distribution curve, and the peak of the distribution, are input data to the network. In return, the network determines one of the Clark levels of ESI, CLII, CLIII, CLIV, or CLV, associated with the melanoma growth stage as output.

Table 3 Specifications of the network and the learning algorithm

	Hidden layer	*Output layer*
Number of neurons	15	5
Activation function	*tansign*	*softmax*
Learning algorithm	Trainlm	
Stopping criterion	1,000 times	
Learning assessment	Mean square error	

5 Experiments and results

As illustrated in the previous sections, data was created by the simulation of the skin's thermal response in a one-month period of melanoma growth. Then, by fitting Gaussian curves on the thermal signals, three suitable features including variance, area under the curve, and the peak of the thermal signal was extracted from the data. These features form the input to the ANN classifier. Table 4 shows the feature vectors for the 30 stage of the tumour growth, 30 seconds after the removal of the cooling.

In Figures 9–13, Gaussian distributions fitted to the thermal signals of five growth stages of melanoma, ESI, CLII, CLIII, CLIV, CLV, are given. The data extracted from the skin surface at y = 1.5 mm, z = 11.6 mm (using Comsol software) clearly shows that the area under the curve, variance and the peak of Gaussian curve are rising by the tumour growth.

Table 4 Feature vector data for 30 stages of melanoma growth, 30 seconds after removal of the cooling

Growth stage	*Variance*	*Area under the curve*	*Peak*
1	0.1105	2.3640e-06	3.39e-05
2	0.1370	1.1855e-04	4.60e-04
3	0.11021	2.5806e-04	9.25e-04
4	0.1464	2.7506e-04	9.80e-04
5	0.5610	2.9217e-04	0.001004
6	0.1596	3.2051e-04	0.001042
7	0.1721	3.3432e-04	0.001055
8	0.1817	3.6972e-04	0.001096
9	0.3099	0.0022	0.014841
10	0.3183	0.0085	0.015297
11	0.3487	0.0113	0.018501
12	0.4265	0.0222	0.029649
13	0.4816	0.0334	0.038742
14	0.5529	0.0528	0.052669
15	0.6041	0.0773	0.066187
16	0.6492	0.0957	0.080156
17	0.6853	0.1153	0.090671
18	0.6937	0.1201	0.093323
19	0.7563	0.1610	0.114154
20	0.7880	0.1849	0.125706
21	0.7878	0.1848	0.125705
22	0.8432	0.2230	0.141656
23	0.8713	0.2378	0.146714
24	0.8955	0.2511	0.150752
25	0.9195	0.2607	0.153104
26	0.9388	0.2674	0.153885
27	0.8713	0.2378	0.146713
28	0.9907	0.2700	0.149184
29	1.0030	0.2635	0.14407
30	1.0330	0.2550	0.136917

Figure 8 Architecture of the designed three-layer neural network (see online version for colours)

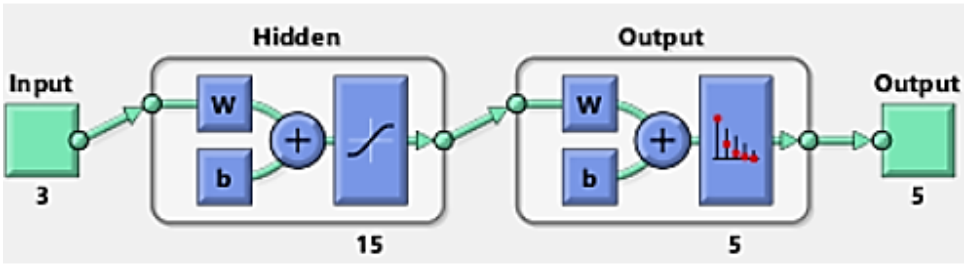

Figure 9 Gaussian curve for ESI (see online version for colours)

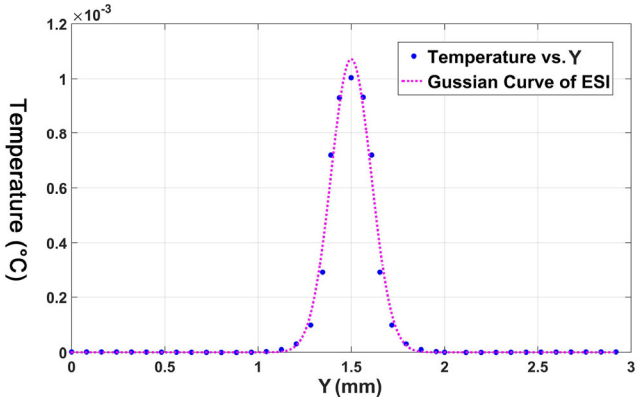

Table 5 The result of ten different trainings of the neural network

Train number	*Accuracy (%)*
1	90.7
2	97.3
3	96.0
4	97.3
5	97.3
6	96.0
7	96.7
8	96.0
9	96.0
10	96.7
Average accuracy	96.0

Figure 10 Gaussian curve for CLII (see online version for colours)

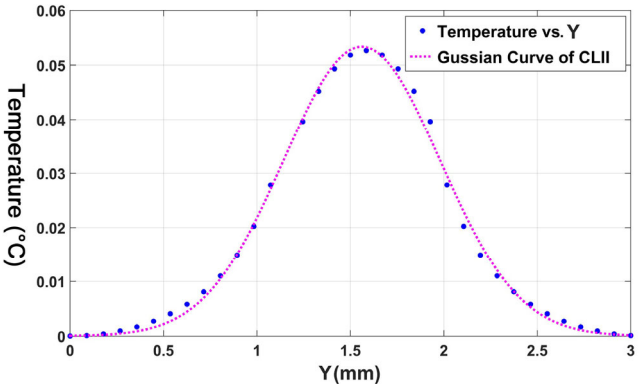

To learn the network model, 70% of the data (selected randomly) is used for training and the rest is used for evaluating the network. To avoid significant categories, data were randomly grouped 20 times, each time, with 70% of data for training and the rest for testing. Then, the neural network is separately trained by a group of training data, and is tested by using the data complementing the training group. Each time, the accuracy of the network is evaluated by the data of the test group. The average accuracy of the learned neural networks obtained during 20 training phases is 96%. Table 4 gives the accuracies (on test data) obtained from ten different full network training runs.

Figure 11 Gaussian curve for CLIII (see online version for colours)

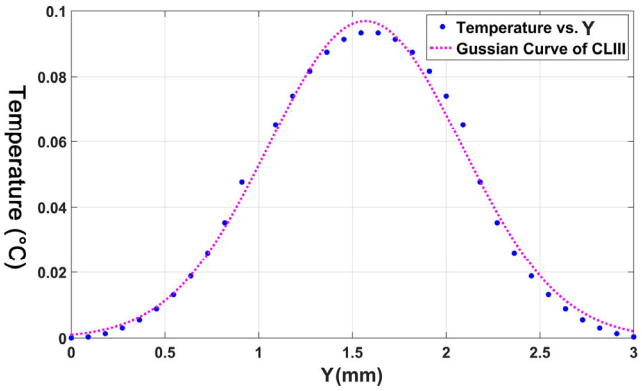

Figure 12 Gaussian curve for CLIV (see online version for colours)

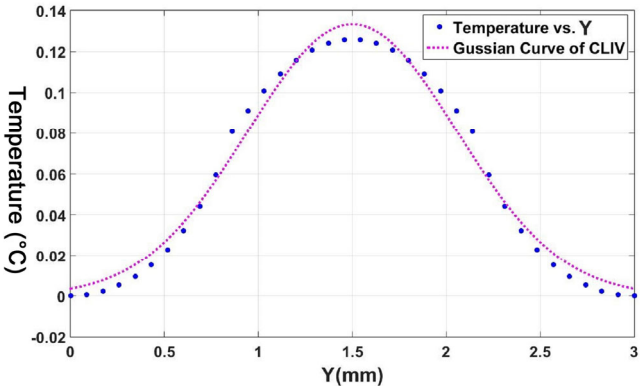

Figure 13 Gaussian curve for CLV (see online version for colours)

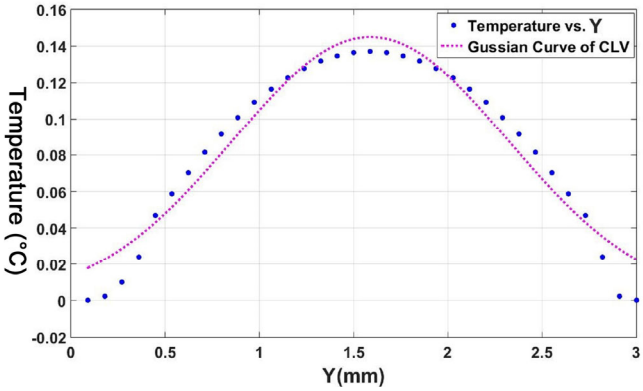

The high accuracy of the network in the level-based classification of the early melanoma shows that the thermal response is a suitable criterion for early diagnosis of the disease. This result provides a quantified validation for the previous studies highlighting the effectiveness of thermal response analysis methods in skin cancer staging task (see e.g., Bhowmik et al., 2014). Also, our results show a remarkable improvement in the accuracy of intelligent melanoma detection systems (see e.g., Mhaske and Phalke,

2013). Also, the efficiency of the selected features of thermal signal distributions is clear from the highly good results achieved.

6 Conclusions

In this paper, we proposed an intelligent melanoma detection system that uses the thermal response difference of the skin to accurately determine the development stage of melanoma. For this purpose, the thermal response of a melanoma in its early growth stages was stimulated numerically using Pennes' heat transfer equation. The temperature distribution differences between the skin surface of the normal tissue and that of the cancerous tissue in each development stage of early melanoma were calculated at the 30th seconds of the heat recovery after the removal of the cold stimulus. Then, features are extracted from the distribution of temperature difference of each growth stage by using Gaussian curve fitting. Finally, a neural network classifier was designed to estimate the growth stage of melanoma. Classification accuracy of 96% shows that the thermal response is an appropriate criterion for detecting the growth stages of melanoma.

References

Agnelli, J.P., Barrea, A.A. and Turner, C.V. (2011) 'Tumor location and parameter estimation by thermography', *Mathematical and Computer Modelling*, Vol. 53, Nos. 7–8, pp.1527–1534.

Anbar, M. (1998) 'Clinical thermal imaging today-shifting from phenomenological thermography to pathophysiologically based thermal imaging', *IEEE Eng. Med. Biol. Mag*., Vol. 17, No. 4, pp.25–33 [PubMed].

Bhowmik, A., Repaka, R. and Mishra, S.C. (2014) 'Thermographic evaluation of early melanoma within the vascularized skin using combined non-Newtonian blood flow and bioheat models', *Computers in Biology and Medicine*, Vol. 53, pp.206–219.

Cetingul, M.P. (2010) *Using High Resolution Infrared Imaging to Detect Melanoma and Dysplastic Nevi*, Dissertation, Johns Hopkins University.

Cetingul, M.P. and Herman, C. (2008) 'Identification of skin lesions from the transient thermal response using infrared imaging technique', *IEEE 5th Int. Symp. on Biomedical Imaging: From Nano to Macro 1–4*, pp.1219–1222.

Cetingül, M.P. and Herman, C. (2010) 'A heat transfer model of skin tissue for the detection of lesions: sensitivity analysis', *Phys. Med. Biol*., Vol. 55, pp.5933–5951.

Çetingül, M.P. and Herman, C. (2011) 'Quantification of the thermal signature of a melanoma lesion', *International Journal of Thermal Sciences*, Vol. 50, pp.421–431.

Dehghan, M. and Sabouri, M. (2012) 'A spectral element method for solving the Pennes bioheat transfer equation by using triangular and quadrilateral elements', *Applied Mathematical Modelling*, Vol. 36, No. 12, pp.6031–6049.

Deng, Z-S. and Liu, J. (2004) 'Mathematical modeling of temperature mapping over skin surface and its implementation in thermal disease diagnostics', *Computers in Biology and Medicine*, Vol. 34, No. 6, pp.495–521.

Elder, D. (1999) 'Tumor progression, early diagnosis and prognosis of melanoma', *Acta Oncol*., Vol. 38, No. 5, pp.535–547, [PubMed].

Herman, C. and Cetingul, MP. (2011) 'Quantitative visualization and detection of skin cancer using dynamic thermal imaging', *Journal of Visualized Experiments: JoVE*, No. 51, pp.e2679–2679, DOI: 10.3791/2679.

Jones, B.F. (1998) 'A reappraisal of the use of infrared thermal image analysis in medicine', *IEEE Trans. Med. Imaging*, Vol. 17, No. 6, pp.1019–1027 [PubMed].

Jones, B.F. and Plassmann, P. (2002) 'Digital infrared thermal imaging of human skin', *IEEE Eng. Med. Bio.*, Vol. 21, No. 6, pp.41–48 [PubMed]

Keangin, P., Wessapan, T. and Rattanadecho, P. (2011) 'Analysis of heat transfer in deformed liver cancer modeling treated using a microwave coaxial antenna', *Applied Thermal Engineering*, Vol. 31, No. 16, pp.3243–3254.

Liu, K-C. (2008) 'Thermal propagation analysis for living tissue with surface heating', *International Journal of Thermal Sciences*, Vol. 47, No. 5, pp.507–513.

Mhaske, H.R. and Phalke, D.A. (2013) 'Melanoma skin cancer detection and classification based on supervised and unsupervised learning', *Int. Conf. on Circuits, Controls and Communications (CCUBE)*, December, pp.27–28.

Qi, Z., Jiaming, Z., Ru, W. and Wei, C. (2008) 'Use of a thermocouple for malignant tumor detection', *Engineering in Medicine and Biology Magazine, IEEE*, Vol. 27, No. 1, pp.6–64.

Singh, S. and Kumar, S. (2014) 'Numerical study on triple layer skin tissue freezing using dual phase lag bio-heat model', *International Journal of Thermal Sciences*, Vol. 86, pp.12–20.

Ströher, G.R. and Ströher, G.L. (2014) 'Numerical thermal analysis of skin tissue using parabolic and hyperbolic approaches', *International Communications in Heat and Mass Transfer*, Vol. 57, pp.193–199.